A FRAMEWORK TO VALIDATE
DIGITAL ROCK TECHNOLOGY

J. Schembre-McCabe, R. Salazar-Tio, G. Ball and J. Kamath
Chevron Energy Technology Company, San Ramon, USA

ABSTRACT

Digital rocks, an emerging technology driven by rapid advances in pore scale 3-D
imaging and computing, is showing promise to reduce cycle time of laboratory
measurements. In order to evaluate this new technology, we have developed a framework
that recognizes both the uncertainty in the input parameters in the numerical
computations and in the measured laboratory data.

3-D images of the rock at sufficient resolution for pore connectivity are first obtained.
We then systematically study the uncertainty of the inputs in the numerical computations
and use Experimental Design to develop a probability range of computed outputs. Next,
we create an uncertainty range for the laboratory measurements, accounting for
measurement errors and techniques. Where there is insufficient information to develop a
suitable range, we use acceptable error criteria specified by the user to develop a range.
The computed and measured ranges are then compared to determine the utility of digital
rocks technology.

We demonstrate the framework using a simple example for single-phase measurements,
primary drainage capillary pressure, and elastic properties. The elements in this workflow
can be extended for other measurements and optimized by using additional information to
reduce uncertainties.

INTRODUCTION

Pore scale numerical modeling has been utilized for two decades, but it is only recently
that the technology became viable for real industry applications due to the improvements
in imaging technology, computational capabilities, and data storage capacity.

One of the essentials in the evolution of any new technology, validation, is listed among
the primary goals of past and current studies (for example, Caubit *et al.* [1]). Our primary
objective is to move from a deterministic comparison of digital computing to
experimental data with a framework that acknowledges the uncertainties in both
computation and measurements. This builds on a framework established for experimental
data by Kamath *et al.* [2].

WORKFLOW

Figure 1 summarizes the typical validation process, which begins with the acquisition of 3D micro-CT scans, followed by image processing and interpretation (segmentation), numerical computation of properties, and analysis of results. Following is an explanation of each step.
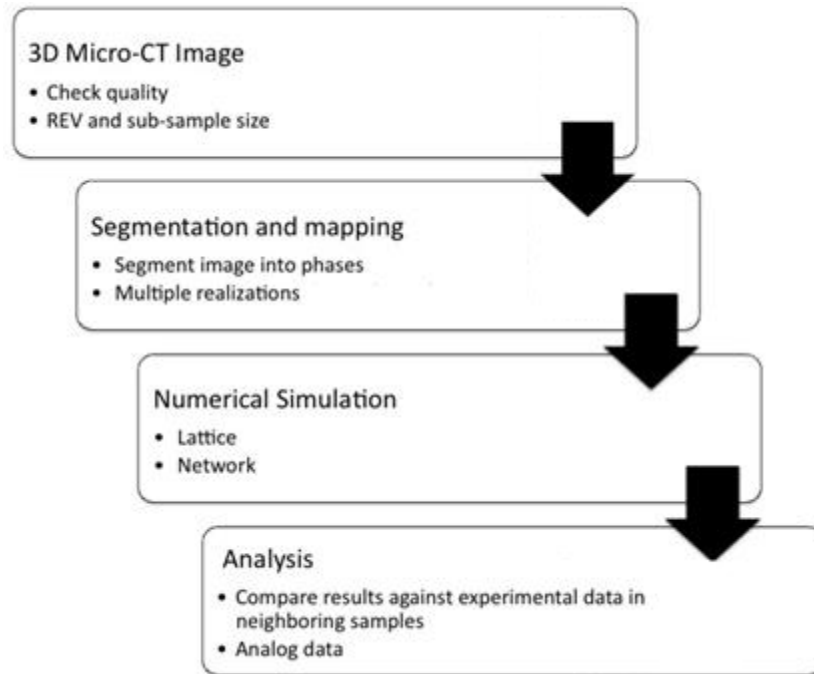
3D Micro-CT Image
- Check quality
- REV and sub-sample size

Segmentation and mapping
- Segment image into phases
- Multiple realizations

Numerical Simulation
- Lattice
- Network

Analysis
- Compare results against experimental data in neighboring samples
- Analog data

Figure 1. General Validation Workflow

Step 1: 3-D micro-CT scans: Resolution and REV

Pore scale modeling of fluid flow properties requires a representation of the pore structure at enough pixel resolution such that the main connected porosity is resolved (μm scale for most of the porous rocks of interest). We accomplish this step by acquiring a 3D image of a mini-plug sample (4-8 mm diameter) using an X-ray micro-tomography scanner. A tomogram is a stack of 2-D images in gray scale, where the intensity represents the X-ray attenuation of the material (proportional to the density). Images are typically noisy, so the stated pixel resolution maybe overshadowed by noise effects [3]. Different scanner setups (X-ray source, camera pixels, magnification system) produce different data set volumes, with typical values: 8-bit or 16-bit 2000^3 pixels and about 2 μm/pixel.

One necessary condition to determine the minimum diameter of the mini-plug sample is that it is large enough to allow a meaningful average over the microscopic heterogeneities at the pore scale. This is called a Representative Elementary Volume (REV). We estimate

the REV size by computing the decay length of statistical spatial correlations for each of the phases: the two-point correlation function and the linear path function. The two-point correlation function is defined as the probability of finding two pixels in the same phase at a given distance. The linear path function is defined as the probability of having a linear segment of a given length completely within one phase. Generally, we prefer to have at least 10 times the largest correlation length for our sample diameter. Another usage of the correlation functions is to validate consistency in the assigned pixel size between different sources of images. For example, with this tool we have found few instances in which the stated X-ray micro-CT pixel size was overestimated when compared to BSEM images.

Step 2: Segmentation
This step consists of assigning a label or phase to each pixel in the 3-D image such that pixels in the same group share characteristics. Clastics could be ideally represented by three components: grain, pore and clay, which can be segmented based on pixel intensity: grain being light, pore being dark and clay being intermediate gray. However, in practice we find that the gray phase is a combination of clay, image resolution limitations, and noise.

Segmentation has been identified as a crucial process in image analysis [4] and its success is related not only to the micro-tomography resolution, but also to the ability to discern and apply appropriate phase classification rules to images with poor signal-to-noise ratio. We use a three-phase based segmentation algorithm that overcome the noise challenge without losing resolution while obtaining pore, grain and intermediate phases**.** Unfortunately, the presence of pores at scale below the image resolution makes the differentiation of phases ambiguous [1, 5, 6]. To help in the segmentation we use higher resolution 2-D imaging like BSEM (Back-scattered Scanning Electron Microscopy), mineralogy imaging like QEMSCAN® (Quantitative Evaluation of Minerals by SCANning electron microscopy), and additional support from QXRD (Quantitative X-Ray Diffraction), and MICP (Mercury Injection Capillary Pressure) to narrow the uncertainty band in the amount and distribution of gray phase. Then, we proceed with selecting different segmentation realizations to quantify the effect of the remaining uncertainty on the numerical results. One important uncertainty is the amount of porosity assigned to the segmented grey (intermediate) phase due to the possible additional contribution of image resolution.

Step 3: Numerical Simulation
The validation exercise practiced on this technology is practically concerned with comparing calculated values against experimental properties, ideally from neighboring samples. Because of the non-uniqueness of image interpretation and criteria involved, we use Experimental Design to optimize the number of numerical simulations to evaluate an often-large array of inputs [7] with the additional advantage of setting the stage to understand the influence of inputs (factors) on the response. In Experimental Design, a

factor is defined as a controlled independent variable; this variable is assigned levels or 'treatment' by the design. These factors are identified in Tables 1 and 2.

Table 1. Factors in lattice-based calculations

Lattice Properties	Factor (s)
Porosity	Segmentation, Gray Phase porosity
Permeability	Segmentation Relaxation parameter (fixed to 1.5)
Formation Factor	Segmentation, Gray Phase Porosity
Drainage Capillary pressure	Segmentation, Gray Phase Porosity
Elastic Properties	Segmentation Shear/Bulk moduli Grain-grain contact
NMR	Segmentation, Gray Phase Porosity Mineral surface relaxivity

Table 2. Factors in Pore network calculations (E-core software)

Pore Network Properties	Factor(s)
Porosity	Segmentation, Gray Phase Porosity
Permeability	Segmentation, Gray Porosity
Formation Factor	Segmentation, Gray Phase Porosity
Drainage Pc, Kr, RI	Segmentation, Gray Phase Porosity Min receding angle Max receding angle Interfacial tension Dip Angle
Imbibition Pc, Kr, RI Fraction oil wet = 0	Segmentation, Gray Phase Porosity Min receding angle Max receding angle Interfacial tension Dip Angle Min WW advancing angle Max WW advancing angle
Imbibition Pc, Kr, RI Fraction oil wet > 0	Segmentation, Gray Phase Porosity Min receding angle Max receding angle Interfacial tension Dip Angle Min advancing angle Max advancing angle Fraction oil wet system Distribution of oil wet pores Hurst Exponent

Table 3 lists the methods used to compute the properties reported in this study, along with the simulation software developer. We perform numerical simulations on the micro-CT original lattice (when calculation is enabled) and on a pore-network simplified representation. Lattice-based calculations are done on large 3-D grids (~1000^3 pixels), and require significant memory and CPU-time, whereas pore-network simulations provide faster results, but could potentially provide less accurate results in samples with significant contribution of gray area or volumes below REV. For the case of two-fluid displacement, we use e-Core software v1.4.5 [8, 9, 10] for the pore-network extraction and simulations. The premise of a pore-network model is that a complex pore structure can be represented by an equivalent network of interconnected pores with the same topological structure, connectivity, and pore/pore-throat size distributions. Several algorithms to create an equivalent pore-network from a micro-CT 3-D image are described by Dong et al. [11].

Table 3. Method used in computation of properties

Properties	Lattice	Pore Network	Method
Porosity	✓	✓	Pore Network[1]
Absolute Permeability	✓	✓	Lattice Boltzmann[1] Pore Network[1]
Formation Factor	✓	✓	Random Walk Pore Network[1]
NMR	✓		Random Walk
Elastic Properties	✓		Finite Element[2]
Drainage Capillary Pressure	✓	✓	Maximal Inscribed Sphere Lattice-Gas Pore Network[1]
Imbibition Capillary Pressure		✓	Pore Network[1]
Drainage/Imbibition Relative Permeability		✓	Pore Network[1]
Drainage/Imbibition Resistivity Index		✓	Pore Network[1]

Step 4: Analysis

(a) For each property, we calculate the computed range [11].

$$\text{range of } x = \bar{x} \pm m\sigma_{\bar{x}} \tag{1}$$

Where, $\bar{x}$ is the mean; $\sigma_{\bar{x}}$ is the standard deviation; the constant **m** is assigned according to the confidence level of the range.

(b) Range for the experimental data is developed using the process described in an earlier paper [2], in which we record experimental values measured for neighboring

---

[1] E-Core, Numerical Rocks; [2] Australia National University

samples (geological variability) using different measurements techniques if available (process uncertainty). Process uncertainty could become significant in two-phase measurements.

(c) Where there are no suitable criteria to develop an experimental range, the user can input an acceptable error band.

(d) The computations are considered to have utility if the computed range is either within the range of the experimental data or within the acceptable error band specified by the user.

WORKFLOW DEMONSTRATION

In this section, we provide a very simple demonstration of the workflow. The uncertainty bands should be considered as an example, and not as an optimized output. There are techniques, such as analysis of sub-volumes and trends that could potentially reduce uncertainty. Table 4 lists the mean values of experimental measurements analyzed in this example, ranges for experimental measurements are estimated using values reported for neighboring samples allocated to different tests in the Special Core Analysis program. The four steps are outlined below.

Table 4. Properties (mean) of sample # 1 analyzed in this study

Porosity, %	22.9
Permeability, mD	990
Formation Factor	13.705
Swir, % $(Pc_{air/brine} = 65\ psia)$	6.9
Elastic Bulk, K (GPa)	13.94
Elastic Shear, G (GPa)	9.81

Step 1: The 3-D micro-CT image of the 5mm diameter mini-plug had 1600x1600x1900 pixels, with a resolution of 2.6 µm/pixel. The estimated correlation length for this rock is about 100 µm (Figure 2), therefore following the criteria described earlier, volumes larger than 380^3 pixels would have sufficient REV to perform lattice and pore network modeling.
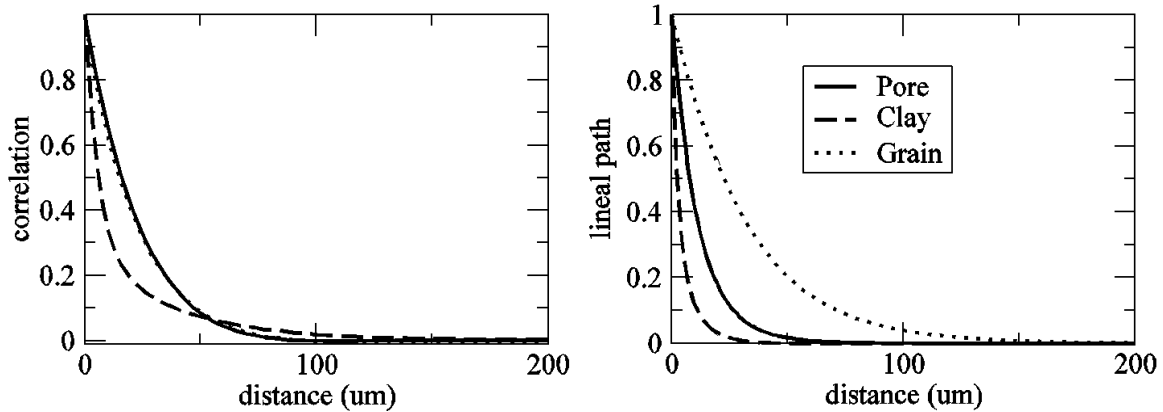
Figure 2: Two-point correlation and lineal path funtion for each phase. We estimate a correlation length for this rock of about 100um.

Step 2: We use the three-phase segmentation approach described earlier for all the simulations; an additional fourth-phase is considered for pixels at the grain-grain contact regions for the elastic simulations. We study two sources of uncertainty: (1) uncertainty due to image interpretation and resolution captured by simulations on large volumes with different segmentations, and (2) Uncertainty due to sample variability captured by simulations on several sub-volumes from one single segmentation realization. We look at the first source of uncertainty in most of the simulations performed in this study; Figure 3 shows the 2 factors in the experimental design: three segmentation realizations in one single large volume of 1100^3 pixels and three values considered for the gray phase in the simulation ($\mu\phi$). For elastic properties, we analyzed the uncertainty due to sample variability, and conducted simulations on five sub-volumes below REV size (300^3 pixels); the size was constrained by limitations in the simulation tool.
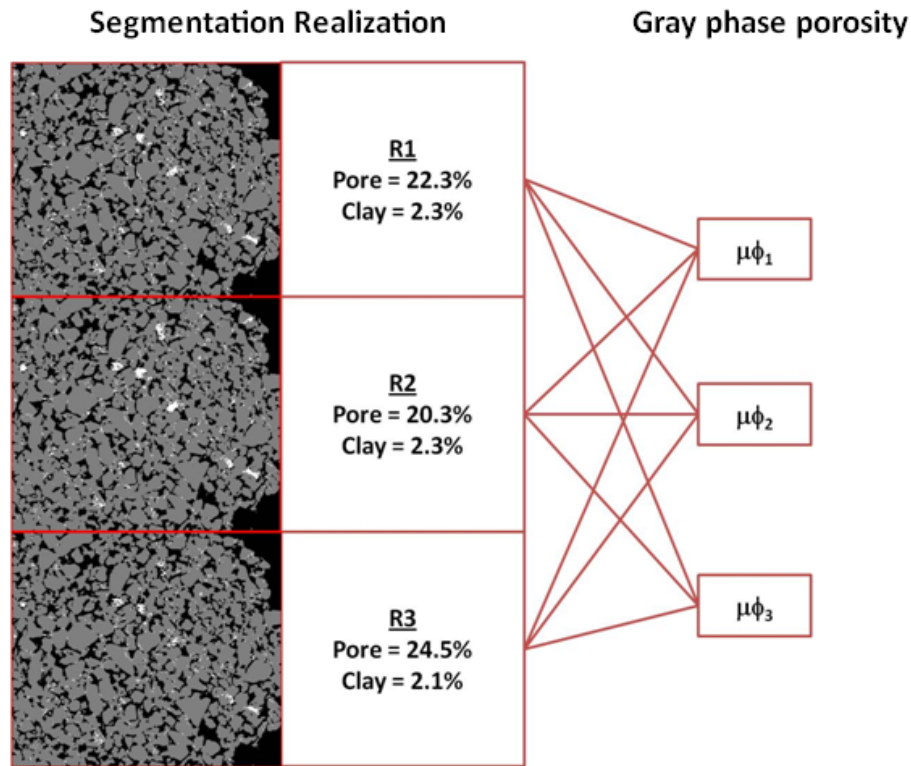
Figure 3. Segmentation and gray phase porosity considered in the Experimental Design.

Step 3: For the analysis of the numerical simulation results, we identified segmentation and gray phase porosity as inputs on a 3-level experimental design [7] and could afford Full Factorial design (3^2). Full Factorial design takes all possible combinations (Figure 3). If the number of combinations in a full factorial design becomes too high to be feasible, fractional factorial design is the preferred choice.

Step 4: Figure 4 illustrates the key elements of this analysis using side-by-side box plots for all groups; solid symbols and lines indicate the distribution average, minimum, and maximum values while the gray box is the 95% confidence around the mean. This information gives some criteria to evaluate the utility of most of the simulation results. A desired situation occur when the simulation 95% range is within the experimental 95% range; in the case shown in Figure 4 this criteria is mostly not met. Notice that in this uncertainty analysis all variability is accounted for as error, while other possible analysis could consider extracting first some meaningful trends or correlations, such that the remaining errors and corresponding uncertainty analysis in the simulations could be further reduced. We could also apply a criterion of user input acceptable error. For example, if a 5% error in porosity is acceptable, the porosity computations can be considered to have utility with 95% confidence.
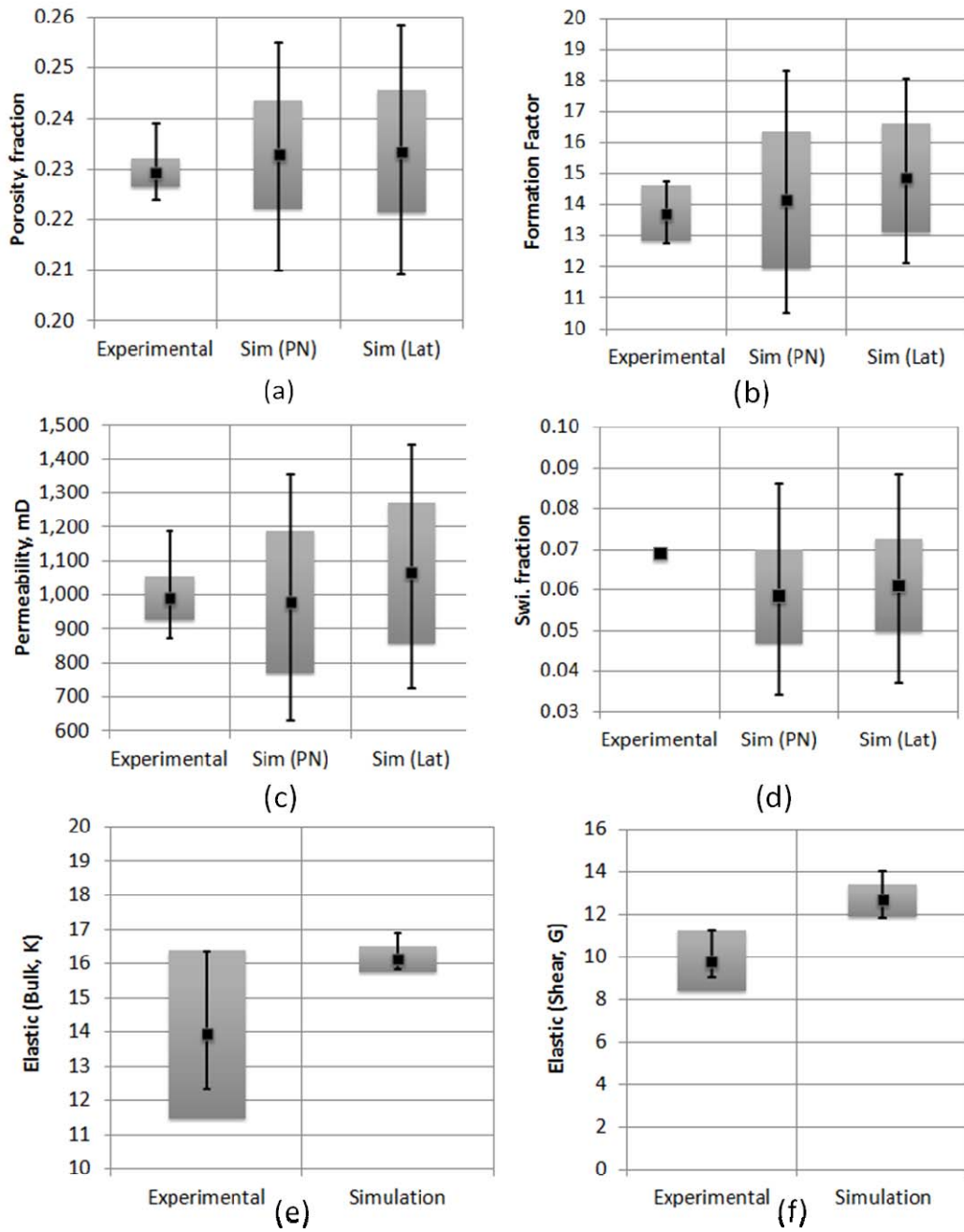
Figure 4. Boxplots for distribution of experimental and numerical values: gray box denote confidence around the mean (solid square) and cap bars indicate low and max values.

We draw attention to the following observations for this particular example:

1. Initial water saturation had a single source of experimental measurement for that particular depth. Thus it does not have distribution around the mean (Figure 4.d). A more rigorous analysis could place an uncertainty around this value if error or range of values is defined by preliminary rock type grouping.

2. In this example, we have good REV for all simulations (except elastic). In addition, there is a comparatively small contribution of gray area so that both lattice and pore-network approaches produce similar results.

3. With exception of elastic properties, experimental data show a narrower band around the confidence interval than computed values and the 95% confidence interval in the computed property overlaps the measurement uncertainty range. These contrasting observations between the first three properties in Figure 4 (porosity, permeability and formation factor) and elastic properties could be caused by the following:

   a. Different design of experiments: Presence of different segmentation realizations for all three first properties (Figure 3) explains the wide uncertainty band around the mean computed values (Figures 4.a, 4.b, and 4.c). In the case of elastic properties, we considered one segmentation realization (which includes grain-grain contact phase) and assigned one set of values to the parameter (Table 5) which might not be most suitable for this rock. The variance in computed values displayed in Figures 4.e and 4.f is due to sample variability since we did not investigate the effect of our choice of input parameters.

Table 5. Input used in Elastic Properties Calculations

Modulus, Gpa	K	G
Pore	2.2	0
Clay	30	15
Grain	37	44
Contacts	3	2

   b. Uncertainty in the experimental measurements: uncertainty in the experimental measurements of the first three properties seems to be lesser than that displayed by elastic properties measurements for this case.

Finally, another important aspect of performing structured sensitivity studies is that we could look at the impact of each input on computed variables by performing analysis of variance (ANOVA). For instance, both microporosity and segmentation affect porosity and irreducible water saturation, whereas permeability is only affected by segmentation realization due to the inherent assumption of non-flow in gray section of the image.

Building on this type of analysis, we could quantify the contribution of each source of uncertainty for better understanding and focus of our work.

SUMMARY
We have described a workflow that can be used to evaluate the utility of digital rock technology. This framework recognizes that the computations have several input parameters that are uncertain and that the measurements have significant imprecision. We demonstrated the workflow using a very simple example. It is possible to optimize the calculations and to extend the workflow to more complex cases, and this will be the subject of later papers.

ACKNOWLEDGMENTS
We thank the Chevron management for supporting this work; Pål-Eric Øren and Mark Knackstedt for access to software and useful discussions; and Chevron, Statoil, and Total E&P USA for permission to publish these results.

REFERENCES
1. Caubit, C., G. Hamon, A. P. Sheppard, and P.E. Øren, "Evaluation of the reliability of Prediction of Petrophysical Data through Imagery and Pore Network Modelling," *Proceedings of the International Symposium of the Society of Core Analysts*, Abu Dhabi (2008), SCA 2008-33.
2. Kamath, J., F. Nakagawa, J. Schembre, T. Fate, E. deZabala, P. Ayyalasomayajula, "Core Based Perspective on Uncertainty in Relative Permeability," *Proceedings of the International Symposium of the Society of Core Analysts,* Toronto (2005), SCA 2005-30
3. Arns, C. K., M. A. Knackstedt, V. W. Pinczewski, and N. S. Martys. "Virtual Permeametry on Microtomographic images." *Journal of Petroleum Sciences Engineering* (2004), **45**, 41-46.
4. Lemmens, H. J. , A. R. Butcher, P. W. S. K. Botha, "FIB/SEM and SEM/EDX: A New dawn for the SEM in the Core Lab?," *Proceedings of the International Symposium of the Society of Core Analysts*, Halifax (2010), SCA 2010-08.
5. Saadatfar, M, M. L. Turner, C. H. Arns, H. Averdunk, T.J. Senden, A. P. Sheppard, R. M.Sok, W. V. Pinczewski, J. Kelly and M.A. Knackstedt, "Rock Fabric and Texture from Digital Core Analysis" *presented at the SPWLA, 46th Annual Logging Symposium, (*2005), New Orleans.
6. Sheppard, A. P, R. M. Sok and H. Averdunk, "Improved Pore Network Extraction Methods," *Proceedings of the International Symposium of the Society of Core Analysts*, Toronto (2005), SCA 2005-20.
7. Montgomery, D., *Design and Analysis of Experiments*, John Wiley and Sons, (2000), 5th Ed.
8. Øren, P. E., S. Bakke, and O. J. Arntzen, "Extending Predictive Capabilities to Network Models," *SPE Journal*, (1998), **3**, 324-336.

9. Øren, P. E. and S. Bakke, "Process Based Reconstruction of Sandstones and Prediction of Transport Properties," *Transport in Porous Media*, 2002, **46**, 311-343.

10. Øren, P. E. and S. Bakke, "Reconstruction of Berea sandstone and pore-scale modeling of wettability effects," *J. Petroleum Science and Engineering* (2003), **39**, 177-199.

11. Dong, H., S. Fjestad, L. Albert, S. Roth, S. Bakke, and P. E. Øren, "Pore Network Modelling on Carbonate: a comparative study of different micro-CT network extraction methods," *Proceedings of the International Symposium of the Society of Core Analysts*, Abu Dhabi (2008), SCA 2008-31.

12. Taylor, J. R., *An Introduction to Error Analysis: The Study of Uncertainties in Physical Measurements*, University Science Books; Sausalito, USA (1996), 2nd edition.